An Increase of Oxidized Phospholipids and the Role of Macrophages in Intraocular Inflammation

Miki Hiraoka[1,2] and Akira Abe[3]

[1]Department of Ophthalmology, School of Medicine, Sapporo Medical University, Sapporo, Hokkaido, Japan
[2]Department of Ophthalmology, Health Sciences University of Hokkaido, Sapporo, Hokkaido, Japan
[3]Department of Molecular Microbiology, Faculty of Life Sciences, Tokyo University of Agriculture, Setagaya, Tokyo, Japan

Correspondence: Miki Hiraoka, 2-5-1 Ainosato Kitaku, Sapporo, Hokkaido 002-8072, Japan; mikihira@nms.ac.jp.

Received: December 11, 2019
Accepted: May 13, 2020
Published: June 11, 2020

Citation: Hiraoka M, Abe A. An increase of oxidized phospholipids and the role of macrophages in intraocular inflammation. *Invest Ophthalmol Vis Sci.* 2020;61(6):23. https://doi.org/10.1167/iovs.61.6.23

Purpose. The present study was conducted to examine the profile of oxidized phospholipids (OxPLs) in uveitis using rat model and clinical specimens, and to elucidate the role of macrophages in the metabolism of OxPLs.

Methods. Lewis rats were immunized with a bovine interphotoreceptor retinoid- binding protein (bIRBP) peptide with complete Freund's adjuvant (CFA) to induce experimental autoimmune uveitis (EAU). The aqueous humor (AH) was collected 2 weeks after immunization. Fifty-four human AH specimens, among which 21 eyes had a history of chronic uveitis, were collected during their cataract surgery. The profile of OxPLs in the AH specimens were analyzed by liquid-chromatography tandem mass spectrometry (LC-MS/MS). In addition, the involvement of macrophages in the viability of cells treated by OxPLs was investigated through a WST-1 assay using ARPE-19 cells and C57BL/6 mouse alveolar macrophages (AMs). The influence of macrophages in the trend of OxPLs was traced by thin layer chromatography (TLC) using AMs.

Results. Six species of OxPLs were detected in the AHs of rats and humans. The content of each OxPL was higher in the uveitis group. Four kinds of OxPLs found in AHs showed cytotoxicity to ARPE-19 cells in a dose-dependent manner. The cytotoxicity was reduced by pretreatment of OxPLs with AMs. When the OxPLs were applied on AMs, a marked reduction of OxPLs in the medium was observed.

Conclusions. The OxPLs formed by intraocular inflammation could induce cytotoxicity. The present findings suggest that the phagocytic macrophages emerging in the inflammation site eliminate OxPLs, and prevent intraocular tissue damage following uveitis.

Keywords: oxidized phospholipids, uveitis, aqueous humor, macrophages, cytotoxicity

Most cases of intraocular inflammation, including uveitis, can be controlled by medicines, such as corticosteroids, with patients usually recovering their vision. However, when the intraocular inflammation is fulminant or uncontrolled for long periods, it usually results in irreversible vision loss even after the uveitis subsides.

There are several reports on how the association of intraocular inflammation with oxidative stress induces cellular signals.[1–3] The oxidized stress following tissue inflammation leads to the production of oxidized phospholipids (OxPLs).[4] In particular, truncated oxidized phosphatidylcholines (OxPCs) production, which are major OxPLs, are known to perturb membrane integrity and barrier properties.[5,6] They also induce apoptosis and cytotoxicity in vitro.[7] The truncated OxPCs are digested by activated macrophages.[8,9] Thus, when the formation of truncated OxPCs exceeds the capacity of digestion in macrophages, unsuitable overproduction of truncated OxPCs may evoke cell damage.

Our previous study revealed that infiltrated macrophages were immuno-positive against the anti-OxPL antibody in experimental autoimmune uveitis (EAU) rats. In addition, it was observed that the infiltrated macrophages highly expressed lysosomal phospholipase A2 (LPLA2).[10] LPLA2 is a degradation enzyme of truncated OxPCs as well as non-oxidized phospholipids.[11] The cell numbers of the infiltrated macrophages immuno-positive for OxPL and LPLA2 in EAU rat ocular sections were parallel with the degree of inflammation,[10] indicating the possibility that LPLA2 is related to OxPL metabolism in the inflammation sites. These findings suggested that the OxPLs formed by the inflammation, such as uveitis, are involved in cell damage in the inflammation sites in the eyes, and that the infiltrated macrophages participate in the metabolism of OxPLs.

In the present study, the formation of OxPCs following intraocular inflammation was investigated by liquid-chromatography tandem mass spectrometry (LC-MS/MS) using an EAU model and clinical specimens. To examine the effect of OxPCs, such as cytotoxicity on ocular cells, four kinds of truncated OxPCs found in the AHs, which are commercially available, were selected. Their effects on ocular epithelial cells were examined using ARPE-19 cells. Additionally, to examine the inhibitory effect of macrophages on the cytotoxicity of those OxPCs against the epithelial cells, mouse alveolar macrophages (AMs) were prepared as a substitute for the infiltrated macrophages at

the site of intraocular inflammation and OxPCs pretreated with AMs were applied on the ARPE-19 cells. The elimination of truncated OxPCs by AMs was also investigated.

Materials and Methods

The present study protocol was approved by the Ethics Committee of the Sapporo Medical University School of Medicine and conducted in accordance with the Declaration of Helsinki. All procedures involving animals were performed in accordance with the ARVO Statement for the Use of Animals in Ophthalmic and Vision Research.

Reagents

Formyl group-truncated OxPCs POBPC, POVPC, and PONPC denote 1-palmitoyl-2-(4'-oxo-butyroyl)-*sn*-glycero-3-PC, 1-palmitoyl-2-(5'-oxo-valeroyl)-*sn*-glycero-3-PC, and 1-palmitoyl-2-(9'-oxo-nonanoyl)-*sn*-glycero-3-PC, respectively. Carboxyl group-truncated OxPCs PMPC, POVPC, and PAzPC denote 1-palmitoyl-2-malonyl-*sn*-glycero-3-PC, 1-palmitoyl-2-glutaryl-*sn*-glycero-3-PC, and 1-palmitoyl-2-azelaoyl-*sn*-glycero-3-PC, respectively. POVPC and PONPC were purchased from Avanti Polar Lipids Corp. (Alabaster, AL, USA), and PGPC and PAzPC were purchased from Cayman Chemical (Ann Arbor, MI, USA).

Induction of Rat EAU

Seven-week-old male Lewis rats (180–220 grams [g]) were obtained from CLEA Japan, Inc. (Tokyo, Japan). All rats were bred and maintained in a specific pathogen-free condition. EAU was induced with its severity scored by the method as described in our previous study.[10] All experiments were performed with 10 animals in 2-week immunization groups.

Collection of Aqueous Humors in Eyes From Rats

Rats were anesthetized with an intraperitoneal injection of a mixture of 0.75 mg/kg of medetomidine, 4 mg/kg of midazolam, and 5 mg/kg of butorphanol.

AHs were obtained by piercing the cornea with a 30-gauge needle and withdrawing the fluid from the anterior chamber. The aqueous humors (AHs) collected from 4 eyes were pooled and centrifuged at 12,000 g for 10 minutes at 4 deg Celsius (°C). The supernatant was used for each assay. All aqueous humor samples were stored at -20°C before each assay. Approximately 10 μl AH was collected from each eye while rats were under anesthesia. The animals were euthanized on the day after AH collection.

Collection of Aqueous Humors in Eyes From Patients With Cataracts

A total of 54 AH specimens were collected from 40 patients (male 10, female 30, age distribution: 50 to 87 years) with senile cataracts, who were recruited from the Department of Ophthalmology, Sapporo Medical University School of Medicine. The details of the samples are as follows: 33 specimens were collected from 23 senile patients with cataracts but without uveitis and 21 came from 17 patients with cataracts forming after uveitis. The cause of uveitis of these patients was not infection. Among the uveitis group, the causes of uveitis included 3 cases with sarcoidosis, 2 cases with Vogt-Koyanagi-Harada disease, 2 cases with Bechet disease, 1 case with human T-lymphotropic virus (HTLV)-1 associated uveitis, 6 cases with unilateral anterior uveitis, and 3 cases with bilateral panuveitis without any cause. Thirteen patients showed granulomatous and four patients showed non-granulomatous uveitis. All patients were treated with topical metamethasone, and some cases received oral prednisolone and intravenous methylprednisolone administration. For the patients with uveitis, the AHs were collected from those free from active inflammation for at least 6 months after treatment with medications. Topical betamethasone was continuously administered to all cases on the day AHs were collected to prevent a relapse of uveitis. The subjects who underwent prior intraocular surgery were eliminated from this study.

After a full explanation of the purpose and protocol for this study was provided to patients, written informed consent was obtained. The AHs were obtained by piercing the cornea with a 26-gauge needle and withdrawing the fluid from the anterior chamber.

Protein Concentration and LPLA2 Activity Measurements

The protein concentration in the AHs was measured using the bicinchoninic acid (BCA) protein assay kit (Pierce, Rockford, IL, USA) with bovine serum albumin as a standard. The LPLA2 activity in AHs was determined by the method as described in our previous study.[12]

Analysis of Truncated Oxidized Phospholipids in Aqueous Humors

To study EAU rats and the clinical specimens, a small amount from each collected AH was used to determine the protein concentration and LPLA2 activity. The rest was immediately frozen using liquid nitrogen and stored at -80°C to prevent oxidation. The patients with cataracts but without uveitis were defined as controls. Patients with cataracts and uveitis were classified as the uveitis group. To compare the profile of truncated oxidized phospholipids between the two groups, five AH samples from each group were selected. To decide which samples to use to perform oxidized phospholipid analysis, we used the protein concentration of each AH sample as a reference. Because the systemic background, such as hypertension and diabetes mellitus, varied among the control group, we chose five samples that showed the close value with the group's average value of AH protein concentration. For the patients with uveitis, we chose the five AH samples with the highest protein concentration from this group. For therapeutic reasons, we hesitated to collect AHs from eyes in a severe inflammatory state.

To identify truncated oxidized phospholipids in the AHs, the frozen samples stored at -80°C were sent to Japan Lipid Technologies (Akita, Japan) and used for LC-MS/MS analysis. In the LC-MS/MS analysis, 1-Heptadacanoyl-lysophoshatidylcholine was used as an internal standard to estimate the content of truncated oxidized phospholipids in the AHs.

In LC-MS/MS analysis, the lipid extract obtained from each AH was subjected to a high sensitive mass spectroscopic analysis through selected reaction monitoring (SRM) with a TSQ Vantage AM LC-MS/MS system (Thermo Fischer

Investigative Ophthalmology & Visual Science

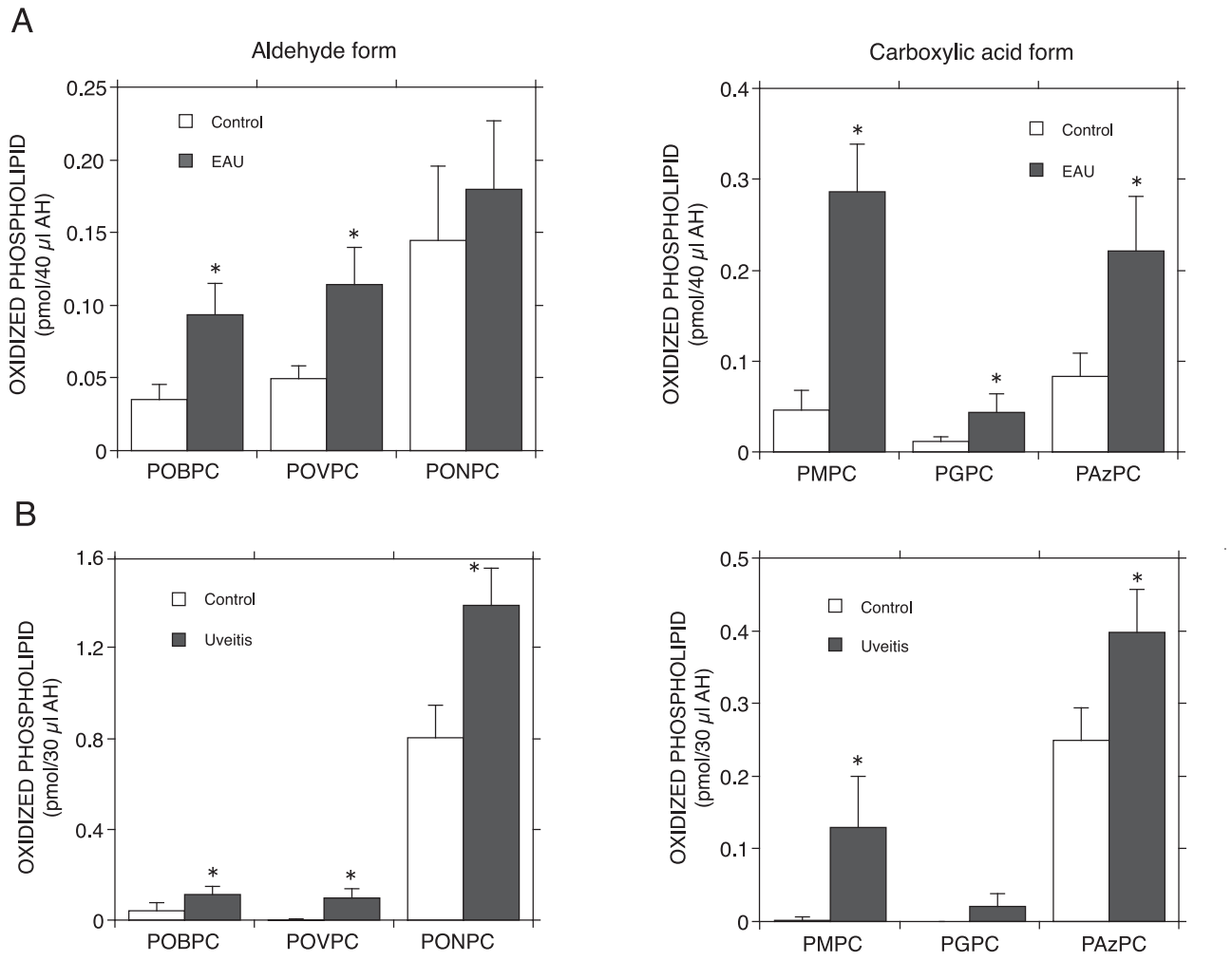

Figure 1. Profiles of OxPCs in the AHs of EAU rats and uveitis patients. (**A**) Rat EAU was induced by an immunized bovine interphotoreceptor retinoid-binding protein (bIRBP) peptide with CFA to 7-week-old Lewis rats. Age-matched rats immunized without bIRBP were used as controls. EAU rats' AHs were collected at 2 weeks after the immunization at the peak of intraocular inflammation. The AHs samples were analyzed by LC-MS/MS (4 rat eyes / sample). Error bars indicate standard deviation ($n = 4$). (**B**) the AHs collected from five senile patients with cataracts but without any ocular diseases and from five patients with cataracts with uveitis were classified as the control and uveitis groups, respectively. Both groups' AHs were analyzed by LC-MS/MS as described in the Materials and Methods. Error bars indicate standard deviation ($n = 5$). Significance was determined using a nonpaired Student's t test. Asterisks indicate significant differences between the control and uveitis groups ($P < 0.05$). Formyl group-truncated OxPCs POBPC, POVPC, and PONPC denote 1-palmitoyl-2-(4'-oxo-butyroyl)-*sn*-glycero-3-PC, 1-palmitoyl-2-(5'-oxo-valeroyl)-*sn*-glycero-3-PC and 1-palmitoyl-2-(9'-oxo-nonanoyl)-*sn*-glycero-3-PC, respectively. Carboxyl group-truncated OxPCs PMPC, PGPC, and PAzPC denote 1-palmitoyl-2-malonyl-*sn*-glycero-3-PC, 1-palmitoyl-2-glutaryl-*sn*-glycero-3-PC, and 1-palmitoyl-2-azelaoyl-*sn*-glycero-3-PC, respectively.

Science). Many oxidized phospholipids come from phosphatidylcholine (PC) having an unsaturated acyl group at the sn-2 position. Hence, in this study, we specifically targeted the oxidized lipids derived from phospholipids having a palmitoyl group at the sn-1 position, a choline as a polar group, and an oleoyl, linoleoyl, arachidonyl, or docosahexanoyl group at the sn-2 position. These phospholipids are converted to oxidized phospholipids having a hydroxyl (-OH), hydroperoxyl (-OOH), formyl (-CHO) or carboxyl (-COOH) group at the sn-2 position by oxidation. We searched for a total of 14 molecular species of oxidized phospholipids predicted from the above PCs. However, we were able to detect and identify only 6 of the 14 species (Fig. 1).

Cell Culture

ARPE-19 Cells. The retinal pigment epithelium cell line ARPE-19 (ATCC No. CRL-2302, American Type Culture collection, Rockville, MD, USA) was grown in DMEM:F12 Medium (Thermo Fisher Scientific, Waltham, MA, USA) supplemented with 10% heat-inactivated fetal calf serum (FCS) and 100 U/mL penicillin/streptomycin at 37°C in a humidified CO_2 (5%) atmosphere.

Mouse Alveolar Macrophages. C57BL/6 mice were obtained from Hokudo (Sapporo, Japan). Lavage fluid was obtained from C57BL/6 mice under anesthesia and alveolar macrophages were collected as previously described.[13] Subsequently, the cell suspension was centrifuged (1200 rpm, 10 minute, 4°C), and cell pellets were then washed with

PBS, collected by centrifugation and suspended in RPMI1640 Medium with 100 U/mL penicillin/streptomycin. The cells were seeded in 24 well plates (1.25×10^5 cells/500 μl/well). After 1 hour of incubation, non-adherent cells were removed by an aspirator, and the adherent AMs were incubated in α-MEM Medium with or without truncated OxPC. The culture supernatant was collected 4 hours later, and centrifuged (10,000 rpm, 10 minutes, 4°C) to remove cell debris. Each resultant supernatant was named as the control AM-treated medium (control medium) or OxPC AM-treated medium (pretreated OxPC medium). In addition, the control medium, pretreated OxPC medium, or control medium supplemented with 30 µM truncated OxPC (control medium + OxPC) was applied to ARPE-19 cells.

WST-1 Viability Assay. To determine the cytotoxic effect of truncated OxPLs on ARPE-19 cells and the role of macrophages, a WST-1 assay was performed according to the manufacturer's protocol (Takara Bio, Shiga, Japan). The ARPE-19 cells were seeded in 96-well plates (8×10^3 cells/100 μl/well) in a culture medium with FCS a day prior to assay. Cells were then washed twice with PBS and incubated with α-MEM Medium. After 1 hour of incubation, the medium was changed to the control medium, the pretreated OxPC medium, or the control medium + OxPC. The cells were cultured for 16 hours. Ten μl/well of Premix WST-1 Reagent was added 1 hour before absorbance measurement. The viability of ARPE-19 cells treated with the control med was defined as 100% (control).

Elimination of Truncated OxPCs From the Medium Cultured With Mouse AMs

Mouse AMs were prepared as described above,[13] suspended in RPMI-1640 Medium and seeded in each well of a 24-well plates (2.5×10^5 cells/well). After 1 hour of incubation, nonadherent cells were removed, and 500 µl of α-MEM medium with 30 µM OxPC was applied. The medium was kept for 0, 1, and 4 hours at 37°C in 5% CO_2, then collected in a small conical tube and centrifuged for 5 minutes at 12,000 g at 4°C. One hundred µl of the resultant supernatant was mixed with 1.9 mL of chloroform/methanol (2:1, v/v) plus 400 µl of 50 mM Na-citrate (pH 4.5) and centrifuged for 5 minutes at 800 g at room temperature. The resultant organic phase was transferred into a glass tube and dried down under a stream of N_2 gas. The dried materials were dissolved with chloroform/methanol (2:1, v/v), applied to an HPTLC plate and developed in a solvent system consisting of chloroform/methanol/water (60:35:8, v/v). To visualize the oxidized PCs, the plate was dried and then soaked in 8% (w/v) $CuSO_4 \cdot 5H_2O$, 6.8% (v/v) H_3PO_4, 32% (v/v) methanol. The uniformly wet plate was briefly dried using a hair dryer and charred for 15 minutes in a 150°C oven. The charred plate was scanned and the contents of each OxPC was estimated by NIH-ImageJ 1.37 version using known amounts of each OxPC as standards.

Removal of Truncated PAzPC by AMs Obtained From Wild-Type or LPLA2 Deficient Mice

$LPLA2^{+/+}$ and $LPLA2^{-/-}$ with C57BL/6 background mice were generated as previously described.[14] No mice were used in more than one study. Mouse AMs were prepared as described above,[14] suspended in RPMI-1640 Medium and seeded in each well of 24-well plates (2.5×10^5 cells/well). After 1 hour of incubation, nonadherent cells were removed, and 500 µl of RPMI-1640 Medium with or without 15 µM PAzPC was applied. The cells were treated for 4 hours at 37°C, 5% CO_2. The medium was then collected in a small conical tube and the cells were washed 3 times with 2 mL of PBS and fixed with 1 mL of cold methanol. The fixed cells were scraped and transferred into a glass tube. Another 1 mL of methanol was used to recover the remaining cells in the well. The 24-well plates were air dried in a Hood.

One milliliter of chloroform was added to the scraped cells in the glass tube and briefly sonicated in a water bath type sonicator. The cell suspension was centrifuged at 2300 g for 30 minutes at 20°C. The resultant supernatant was transferred into a glass tube, dried down under a stream of nitrogen gas, and stored at -20°C as the cellular lipid fraction. The cell pellet was air dried in a hood and stored at room temperature as the cellular protein fraction. The cellular lipid fraction was re-dissolved with 3 mL of chloroform/methanol (2:1, v/v) and partitioned by centrifugation at 800 g for 5 minutes at 20°C following the addition of 0.8 mL of 50 mM Na-citrate (pH 4.5). The organic layer was collected and used for thin layer chromatography (TLC) analysis. To determine the PAzPC concentration in the medium, 0.4 mL of the collected medium was mixed with 3 mL of chloroform/methanol (2:1, v/v) plus 0.4 mL of 50 mM Na-citrate (pH 4.5) and partitioned by centrifugation at 800 g for 5 minutes at 20°C. The resultant organic layer was collected and used for TLC analysis. The content of the OxPCs was determined as described above.

For protein determination, the cell-protein fraction was treated with 1 mL of 0.2 N NaOH in a water bath type sonicator and the insoluble materials were removed by centrifugation. Additionally, 1 mL of 0.2 N NaOH was added to each well of the dried 24-well plates. The plates were gently shaken for 2 hours at room temperature. The NaOH solutions (the cell-protein fraction's NaOH plus the dried well's NaOH) were used to determine the cell-protein content in each well by means of a BCA assay.

Statistical Analysis

All results are expressed as mean ± standard deviation (SD). The values were processed for statistical analyses (unpaired Student's *t*-test).

Results

Truncated Oxidized Phosphatidylcholines in AHs of EAU Rats and Patients With Uveitis

The protein level of the AHs reflect the extent of inflammation.[10,15,16] As shown in our previous study, 2 weeks after the immunization was the time point of peak inflammation in our system. In the current study, 18 eyes showed a score of 2 and two eyes showed a score of 3. The LPLA2 activity in the AH was also significantly higher in the rat EAU group than in the control group.[10]

Through LC-MS/MS analysis, six different species of truncated oxidized phosphatidylcholines (OxPCs), POBPC, POVPC, PONPC, PMPC, POVPC ,and PAzPC, were detected in the AHs (Fig. 1A). The truncated OxPCs were estimated to be PC molecules containing a short acyl chain with the formyl or carboxyl group at the sn-2 position from their

Investigative Ophthalmology & Visual Science

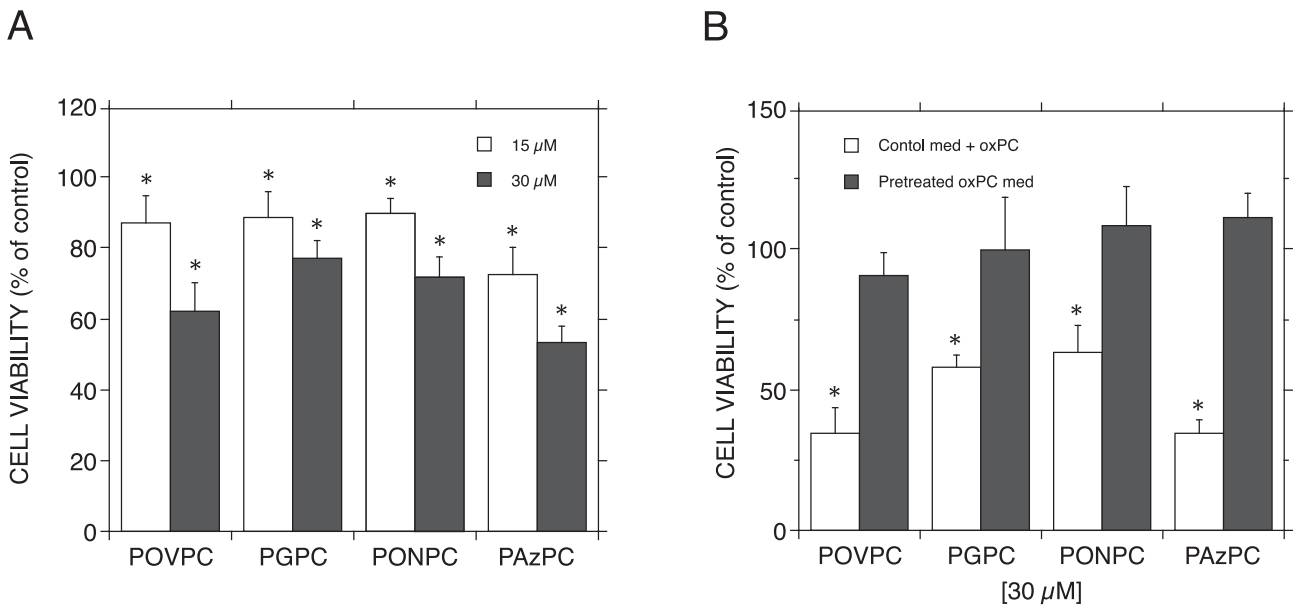

Figure 2. Effect of truncated oxidized phosphatidylcholines on ARPE-19 cells. (**A**) ARPE-19 cells were treated with 15 μM or 30 μM of four different truncated OxPCs, POVPC, PGPC, PONPC, and PAzPC, for 16 hours at 37°C as described in the Materials and Methods. After the treatment, a WST-1 assay was applied to determine the cytotoxicity through OxPC treatment. Error bars indicate standard deviation ($n = 5$). The viability of ARPE-19 cells treated without OxPC was defined as 100% (control). (**B**) The control medium indicates a culture supernatant of mouse AMs. Control medium + OxPC indicates that 30 μM OxPC was added when the control medium was applied to ARPE-19 cells. The pretreated OxPC medium indicates that OxPC was incubated on AMs for 4 hours, and the resultant supernatant was then applied to ARPE-19 cells. The viability of ARPE-19 cells treated with the control medium was defined as 100% (control). Error bars indicate standard deviation ($n = 5$). Significance was determined using a nonpaired Student's *t*-test. Asterisks indicate significant differences against the control medium ($P < 0.01$). **A** and **B** represent two independent experiments.

molecular masses. Each OxPC level in the AH was higher in the EAU group (2 weeks after immunization) than in the control group (Fig. 1A).

Among the AHs of the clinical samples, those obtained from the uveitis group showed higher values than the control group for protein concentration (11.48 ± 2.007 mg/mL vs. 5.93 ± 0.949 mg/mL) and LPLA2 activity (12.14 ± 2.104 nmol/h/mL vs. 6.13 ± 0.941 nmol/h/mL). The analyzed patients in the uveitis group did not present apparent cellular infiltration in the anterior chamber, but their AHs showed a high protein concentration. It is likely that their eyes were in a state of mild but chronic inflammation.

LC-MS/MS analysis indicated that with the exception of PGPC in the control group, the AHs obtained from both groups contained six truncated OxPCs, shown in the EAU study to be truncated oxidized phospholipids (Fig. 1B). Each truncated OxPC level in the AH was higher in the uveitis group than in the control group (Fig. 1B).

Effect of Truncated OxPCs on ARPE-19 Cells

Cytoxicity of Truncated OxPCs on ARPE-19 Cells. Among the six species of truncated OxPCs found in the AHs, four were commercially available. To understand the effect of truncated OxPCs on ocular epithelial cells, ARPE-19 cells, which are human retinal epithelium cells, were chosen and treated with 4 different species of OxPCs, POVPC, PGPC, PONPC, and PAzPC, for 16 hours. All tested OxPCs expressed cytotoxicity on ARPE-19 cells (Fig. 2A). In another experiment, the cell viability values of ARPE-19 cells with 15 μM OxPCs were as follows: POVPC = 49.4 ± 9.36%; PGPC = 69.0 ± 17.10%; PONPC = 58.2 ± 8.75%, and PAzPC = 68.5 ± 26.02%. The cell viability values with 30 μM OxPCs were as follows: POVPC = 26.2 ± 7.15%; PGPC = 41.0 ± 5.28%; PONPC = 51.7 ± 8.63%, and PAzPC = 51.8 ± 21.15% (SD [n = 6]). As expected, 30 μM of the OxPCs showed cytotoxicity higher than 15 μM. To observe the effect of those OxPCs on the cells, the concentration of truncated OxPC was fixed at 30 μM for the remainder of the experiments using ARPE-19 cells.

We also examined the cytotoxicity of PGPC and PAzPC on alveolar macrophages. When the macrophages were treated with 30 μM OxPCs for 4 hours, the cell viability was reduced by 31.4.4 ± 5.30% and 63.6 ± 7.27%, respectively. Errors were SD ($n = 6$), $P < 0.005$.

Detoxification of Truncated OxPCs by Mouse AMs. The cytotoxicity was induced by the control medium supplemented with 30 μM OxPC (control medium + OxPC in Fig. 2B). When α-MEM Medium containing OxPCs was pretreated for 4 hours with mouse AMs, the supernatant lost the cytotoxicity on ARPE-19 cells completely (pretreated OxPC med in Fig. 2B). There was no significant difference between the "control medium" and "pretreated OxPC medium." The cytotoxicity was induced by the control med supplemented with 30 μM OxPC (control medium + OxPC in Fig. 2B). The α-MEM medium preincubated for 4 hours at 37°C with 30 μM OxPC but not AM reduced the viability of ARPE-19 cells as follows: POVPC = 25.1 ± 4.24%; PGPC = 44.2 ± 11.9%; PONPC = 65.8 ± 7.96%, and PAzPC = 47.3 ± 11.8% (SD [$n = 5$]). These cytotoxicities were similar to those seen with the control medium + OxPC in Fig. 2B. This showed that the preincubation of OxPCs without AMs did not reduce its cytotoxic effect. In addition, we could not observe new production of either 1-palmitoyl-2-

Investigative Ophthalmology & Visual Science

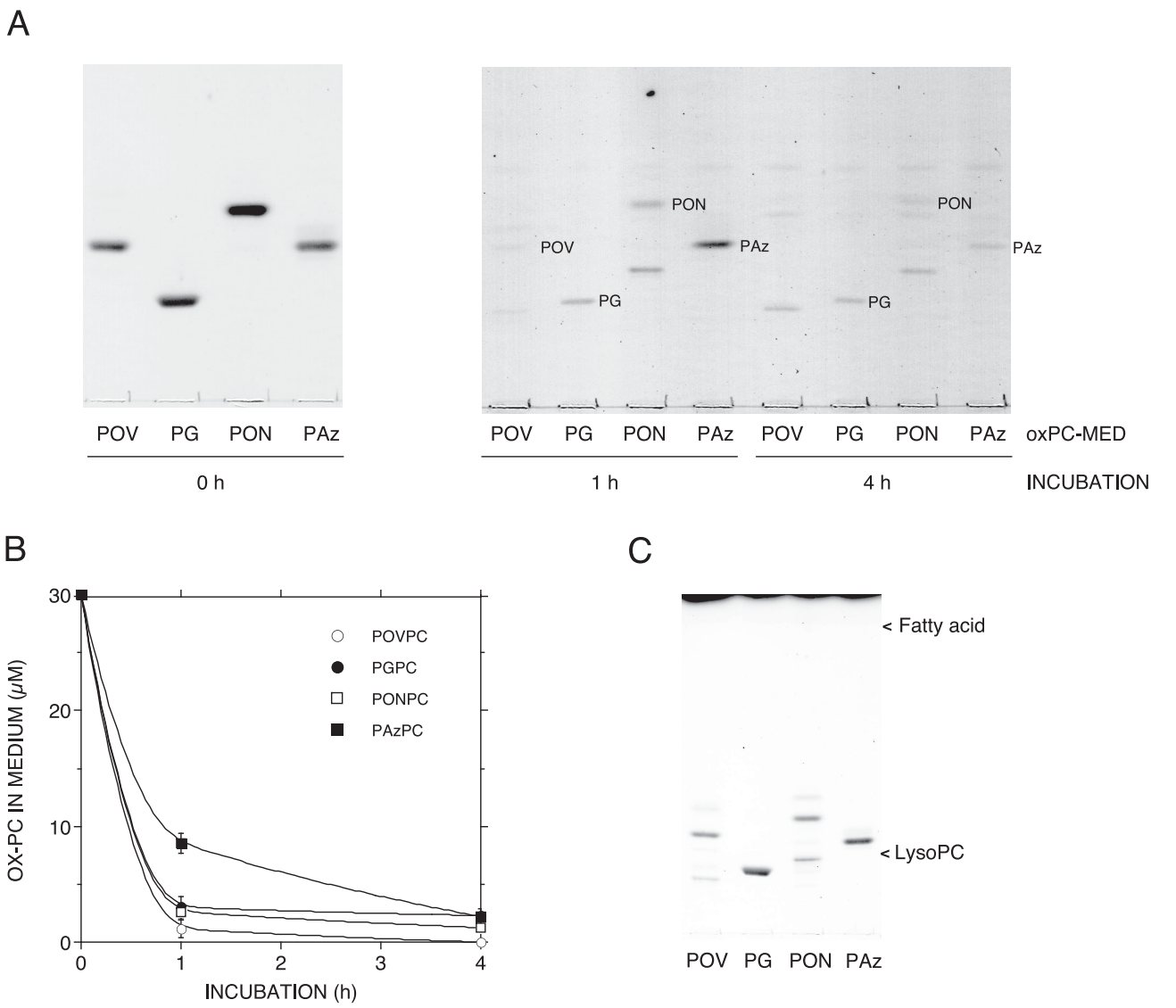

Figure 3. Elimination of truncated oxidized phosphatidylcholine in the medium by mouse AMs. Four different kinds of 30 μM truncated OxPCs such as POVPC (POV), PGPC (PG), PONPC (PON), and PAzPC (Paz) were treated with mouse AMs for 1 and 4 hours at 37°C. The truncated OxPC found in the medium at each time point is shown by TLC (**A**) and quantified as described in the Materials and Methods. The truncated OxPC concentration in the medium at different time points was plotted against the incubation time (**B**). The OxPC concentrations in the cell and medium were determined from three different cultures. Error bars indicate standard deviation ($n = 3$). The values of Rf for POVPC, PGPC, PONPC, and PAzPC on the plate were 0.39, 0.24, 0.46, and 0.38, respectively. (C) Individual OxPCs were treated with the medium without mouse AMs for 4 hours at 37°C. The truncated OxPC found in the medium is shown by TLC (**C**). Little lyso-PC or fatty acid was detected in this study.

lyso-PC or palmitic acid in the pre-incubated medium by TLC analysis although a portion of POVPC or PONPC was converted to several unknown compounds (Fig. 3C). POVPC and PONPC have an aldehyde group that is reactive against amino compounds in the medium. Thus, a portion of those aldehyde-OxPCs must have been converted to the unknown compounds during the 4 hours of incubation. This indicates that the hydrolysis of each OxPC by the medium was insignificant.

In addition, a marked reduction of the concentration of OxPCs in the supernatant after treatment of the medium with AMs (Fig. 3A, B) could be observed. These results suggested that the detoxification of OxPCs by AMs is due to the elimination of OxPCs from the cultured medium by AMs.

We also examined the detoxification of PGPC and PAzPC by ARPE-19 cells. ARPE-19 cells were incubated in an α-MEM medium with or without 30 μM OxPCs for 4 hours in 24-well plates at a similar cell confluency to AMs. The culture supernatant was collected and applied on ARPE-19 cells in 96-well plates and incubated for 16 hours. The cell viability values of the control medium added to OxPC were as follow: 32.8 ± 4.67% for PGPC and 33.6 ± 4.60% for PAzPC. The cell viability values of OxPC preincubated medium were as follow; 85.5.8 ± 7.19% for PGPC and 60.5 ± 10.80% for PAzPC. Errors were SD ($n = 6$), $P < 0.005$.

Investigative Ophthalmology & Visual Science

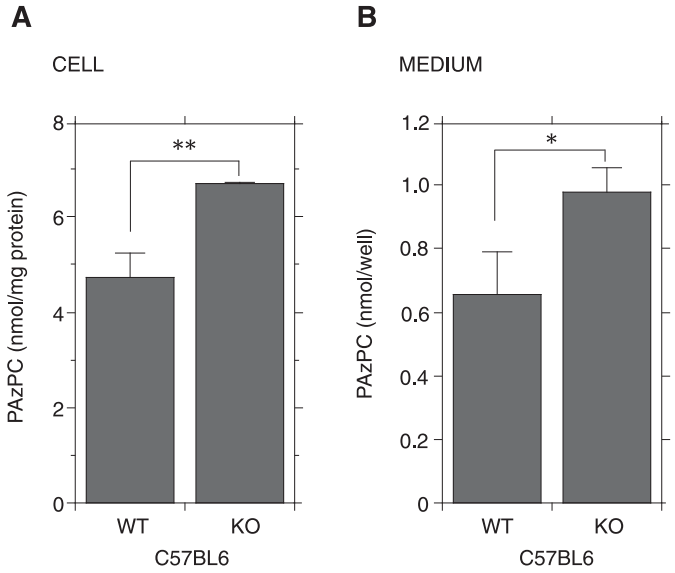

Figure 4. Removal of PAzPC by mouse AMs obtained from wild-type and LPLA2 deficient mice. The cell culture, lipid, and protein analyses were carried out as described in the Materials and Methods. The cells (2.5×10^5 per well) were treated in the presence or absence of 15 µM PAzPC. After the treatment for 4 hours, the media were collected and 100 µl was immediately used for lipid analysis. The PAzPC content in the medium is shown in the right panel. Error bars indicate standard deviation ($n = 3$). The cells were washed with PBS, fixed with methanol, and used for protein and lipid analysis. The PAzPC content in the cell is shown in the left panel. Error bars indicate standard deviation ($n = 3$). Significance was determined using a nonpaired Student's *t*-test. Asterisks indicate significant differences between the wild-type and LPLA2 deficient cells (*$P < 0.05$, **$P < 0.01$). Similar results were also obtained from another independent experiment. WT and KO denote wild-type and LPLA2 deficient mice, respectively.

Removal of Truncated OxPC by AMs Prepared From Wild-Type or LPLA2 Deficient Mice

Recently, we found that LPLA2 preferentially hydrolyzed truncated OxPCs in vitro.[11] This study also showed that LPLA2-overexpressed CHO cells more efficiently catabolize PAzPC in the cultured system than CHO cells. To determine whether LPLA2 is connected with the metabolic pathway of truncated OxPCs by AMs, mouse AMs were prepared from both wild-type and LPLA2 deficient C57BL6 mice

Alveolar macrophages of LPLA2 deficient mice develop phospholipidosis due to the reduction of phospholipid digestion.[14] PAzPC has a carboxyl group but not an aldehyde group, and is relatively more stable in a culture medium than other truncated OxPCs. Thus, it was suitable to trace the trend of truncated OxPCs in this study. The AMs were incubated with 15 µM PAzPC for 4 hours. As shown in Fig. 4, the PAzPC content in the wild-type cells was significantly lower than that in the LPLA2 deficient cells. In addition, the PAzPC concentration in the wild-type cell cultured medium was significantly lower than that in the LPLA2 deficient cell cultured medium (Fig. 4). In our preliminary study using AMs, when the cells (two different cultures) were treated with 15 µM PAzPC for 1, 2, and 4 hours, the content of PAzPC in both the cell and medium was reduced in a time-dependent manner. If the mean value of PAzPC level at 1 hour after the treatment is defined as 1, those at 2 hours and 4 hours were 0.91 and 0.57, respectively, in the cell and 0.61 and 0.27, respectively, in the medium. These results suggested that intracellular LPLA2 of the macrophages partially contributes to the degradation and detoxification of truncated OxPCs.

Discussion

In recent years, the prognosis of uveitis has improved alongside advances in the development of immunosuppressive medicine. However, insufficient control of uveitis can result in irreversible visual impairment. The main causes of these malfunctions are retinal disorder and glaucoma.[17] Retinal photoreceptor cell damage in particular can lead to permanent vision loss. OxPC was detected in the photoreceptor and retinal pigment epithelium of the macular area. The levels of OxPCs increase through aging, and the intensive production of OxPCs was observed in the macula of age-related macular degeneration (AMD) in humans.[18] Subretinal OxPL injection has been shown to induce choroidal neovascularization (CNV) by means of mimicking human AMD in mice.[19] These findings suggest that an abundance OxPLs can introduce disruption in retinal cells.

OxPLs are mainly ingested by macrophages and neutrophils.[20] Substantial OxPL production following infection inhibits bacterial phagocytosis by macrophages.[21,22] Once the mass of truncated OxPCs exceeds the detoxification ability of macrophages, their cytotoxicity may be unavoidable. The accumulation and long-term exposure of truncated OxPCs in the eye could contribute to intraocular cell damage. Thus, the phagocytic macrophages emerging during inflammation must ingest and digest the OxPC-conjugated cells and cell debris to terminate the inflammation.

In the present study, LC-MS/MS measurements of EAU rats and patients with uveitis revealed that the production of six species of truncated OxPCs found in AHs from both animal models and clinical samples was higher in the intraocular inflammation groups than in the control groups

(Fig. 1). At this stage, we cannot rule out the possibility that the differences observed between the control and uveitis conditions were due to a lack of antioxidants in AH samples. However, in both the control and uveitis sample assays, the samples were processed and analyzed under conditions as similar as possible. The values of individual truncated oxidized PCs obtained from the control group were statistically analyzed and showed values significantly higher than those obtained from the uveitis group, except for PAzPC and PGPC in rats and humans, respectively. Therefore, the present results are thought to support the idea that there is a significant correspondence between truncated oxidized PC formation and uveitis.

All patients with uveitis received topical betamethasone administration at the time of AH collection. It is impossible to eliminate the possible influence of corticosteroid treatment in the oxidized phospholipids profiles of the AHs. It has been reported that such systemic betamethasone administration can lead to an increase of disaturated phosphatidylcholine in lamellar bodies of rat lungs.[23] However, disaturated phosphatidylcholine cannot be a precursor of oxidized phospholipids. To address this issue, further study is necessary to examine the clinical AH samples from patients with cataracts without any other ocular diseases who have received topical betamethasone. Because EAU rats without any treatment and the uveitis group showed similar patterns in the oxidized phospholipids profile, it is likely that the intraocular inflammation led to these changes. Our data indicate that the intraocular inflammation may enhance the production of truncated OxPCs. Several OxPCs including POVPC, PGPC, PONPC, and PAzPC were detected in the human vitreous.[24] The OxPCs production may enhance during posterior uveitis or pan uveitis.

Some types of truncated OxPCs, such as POVPC, PGPC, PONPC, and PAzPC, have been known to express cytotoxicity.[7,9] For example, exogenous OxPCs are rapidly internalized in mammalian cells and induce cytotoxicity.[25] Our study showed that all tested truncated OxPCs have cytotoxicity on human retina epithelial ARPE-19 cells (Fig. 2A).

In our previous study, the immuno-histochemical examination of rats at 2 weeks after EAU immunization showed the numerous oxidized phospholipid localizations found on infiltrated macrophages.[10] This implied that those macrophages are probably associated with ingestion and digestion of truncated OxPCs produced during inflammation.

In EAU, macrophages and microglial cells are known to enhance the responses of uveitogenic T cells and induce the destruction of photoreceptors and retinal tissues. It has been also reported that the macrophage depletion can delay the onset and reduce the severity of EAU.[26] In contrast, infiltrating macrophages are known to change their properties during the course of EAU. The macrophages at the peak of inflammation have the characteristics of IFN-γ primed, TNF-α activated macrophages, and the macrophages during resolution show the characteristics of TGF-β, anti-inflammatory cytokine, primed cells.[27] It is thought the infiltrated macrophages at inflamed tissue change their properties involving from cell damage to repair.

Macrophages are known to play an important role in the oxidized phospholipids metabolism at inflammatory sites, such as atherosclerosis. Thus, we conducted the current experiment to study the role of macrophages in intraocular inflammation.

The present study showed that treatment of truncated OxPCs with mouse AMs eliminates the cytotoxicity on ARPE-19 cells caused by those OxPCs (Fig. 2B). In addition, it was found that the AMs markedly reduce the concentrations of truncated OxPCs in the medium (Fig. 3A, B). The RPE cells are known to have phagocytic activity. In our experiments, ARPE-19 cells showed detoxification of truncated OxPCs. It is difficult to compare the detoxification ability between ARPE-19 cells and AMs because of the cell type differences between adherent fibroblast and hematopoietic cells. From our results, it appears that AMs are more susceptible to OxPCs than ARPE-19 cells. However, AMs could reduce the cytotoxicity by OxPCs completely. It can be speculated that infiltrated macrophages have a higher capacity to remove OxPCs than RPE during intraocular inflammation.

In the EAU model, a similar immuno-histochemical staining pattern was observed between OxPL and LPLA2.[10] LPLA2 is a phospholipase enzyme with pH optimum at an acidic condition for non-oxidized phospholipids. In contrast, OxPCs show preferential hydrolysis by LPLA2 more efficiently compared to those of non-oxidized phospholipids.[11] Furthermore, the lack of LPLA2 leads to the development of phospholipids accumulation in AMs with lamellar inclusion bodies.[14] Thus, we performed our study to examine the involvement of LPLA2. The LPLA2 deficient AMs significantly reduced the ability of degradation of truncated OxPC PAzPC in both cellular and medium fractions in the cultured system (Fig. 4). Despite this, we observed that the AMs isolated from LPLA2 deficient mice were able to eliminate the cytotoxicity of truncated OxPCs as the AMs from wild type mice (data not shown). It is likely that the LPLA2 deficient AMs must have bypassed route(s) to metabolize truncated OxPCs by other phospholipases.

Taken together, we propose that the activated phagocytic cells infiltrated at the inflammation site could play an important role toward the elimination and detoxification of truncated OxPCs produced during the intraocular inflammation. Such a clearance system may protect the intraocular tissues from injury. However, either by the overproduction of the truncated OxPCs following severe inflammation or by malfunction of activated macrophages, potentially resulting in visual dysfunction. In such a situation, LPLA2 and other phospholipases may contribute to the catabolism of truncated OxPCs formed at ocular inflammation site and assist in ceasing the risk of cell damage in ocular tissues. It assumes that controlling the phospholipids oxidation makes it possible to maintain a favorable retinal function.

Acknowledgments

The authors thank James A Shayman from the University of Michigan for providing LPLA2 deficient mice. In addition, we would like to express our appreciation to Hiroshi Ohguro in the Department of Ophthalmology at Sapporo Medical University for his financial support.

Supported by a grant from the Japan Society for the Promotion of Science (JSPS KAKENHI; Grant number: 18K09452).

Disclosure: **M. Hiraoka,** None; **A. Abe,** None

References

1. Bochkov VN, Oskolkova OV, Birukov KG, Levonen AL, Binder CJ, Stöckl J. Generation and biological activities

Investigative Ophthalmology & Visual Science

of oxidized phospholipids. *Antioxid Redox Signal*. 2010;12:1009–1059.
2. Kadl A, Sharma PR, Chen W, et al. Oxidized phospholipid-induced inflammation is mediated by Toll-like receptor 2. *Free Radic Biol Med*. 2011;51:1903–1909.
3. Greig FH, Kennedy S, Spickett CM. Physiological effects of oxidized phospholipids and their cellular signaling mechanisms in inflammation. *Free Radic Biol Med*. 2012;52:266–280.
4. Fruhwirth GO, Loidl A, Hermetter A. Oxidized phospholipids: from molecular properties to disease. *Biochim Biophys Acta*. 2007;1772:718–736.
5. Sabatini K, Mattila JP, Megli FM, Kinnunen PK. Characterization of two oxidatively modified phospholipids in mixed monolayers with DPPC. *Biophys J*. 2006;90:4488–4499.
6. Beranova L, Cwiklik L, Jurkiewicz P, Hof M, Jungwirth P. Oxidation changes physical properties of phospholipid bilayers: fluorescence spectroscopy and molecular simulations. *Langmuir*. 2010;26:6140–6144.
7. Fruhwirth GO, Moumtzi A, Loidl A, Ingolic E, Hermetter A. The oxidized phospholipids POVPC and PGPC inhibit growth and induce apoptosis in vascular smooth muscle cells. *Biochim Biophys Acta*. 2006;1761:1060–1069.
8. Vladykovskaya E, Ozhegov E, Hoetker JD, et al. Reductive metabolism increases the proinflammatory activity of aldehyde phospholipids. *J Lipid Res*. 2011;52:2209–2225.
9. Stemmer U, Dunai ZA, Koller D, et al. Toxicity of oxidized phospholipids in cultured macrophages. *Lipids Health Dis*. 2012;11:110.
10. Ohkawa E, Hiraoka M, Abe A, Murata M, Ohguro H. Fluctuation of lysosomal phospholipase A2 in experimental autoimmune uveitis in rats. *Exp Eye Res*. 2016;149:66–74.
11. Abe A, Hiraoka M, Ohguro H, Tesmer JJ, Shayman JA. Preferential hydrolysis of truncated oxidized glycerophospholipids by lysosomal phospholipase A2. *J Lipid Res*. 2017;58:339–349.
12. Hiraoka M, Abe A, Inatomi S, Sawada K, Ohguro H. Augmentation of lysosomal phospholipase A2 activity in the anterior chamber in glaucoma. *Curr Eye Res*. 2016;41:683–688.
13. Abe A, Hiraoka M, Wild S, Wilcoxen SE, Paine R, 3rd, Shayman JA. Lysosomal phospholipase A2 is selectively expressed in alveolar macrophages. *J Biol Chem*. 2004;279:42605–42611.
14. Hiraoka M, Abe A, Lu Y, et al. Lysosomal phospholipase A2 and phospholipidosis. *Mol Cell Biol*. 2006;26:6139–6148.
15. Shah SM, Spalton DJ, Taylor JC. Correlations between laser flare measurements and anterior chamber protein concentrations. *Invest Ophthalmol Vis Sci*. 1992;33:2878–2884.
16. Whitcup SM, DeBarge LR, Rosen H, Nussenblatt RB, Chan CC. Monoclonal antibody against CD11b/CD18 inhibits endotoxin-induced uveitis. *Invest Ophthalmol Vis Sci*. 1993;34:673–681.
17. Dick AD, Tundia N, Sorg R, et al. Risk of ocular complications in patients with noninfectious intermediate uveitis, posterior uveitis, or panuveitis. *Ophthalmology*. 2016;123:655–662.
18. Suzuki M, Kamei M, Itabe H, et al. Oxidized phospholipids in the macula increase with age and in eyes with age-related macular degeneration. *Mol Vis*. 2007;13:772–778.
19. Suzuki M, Tsujikawa M, Itabe H, et al. Chronic photo-oxidative stress and subsequent MCP-1 activation as causative factors for age-related macular degeneration. *J Cell Sci*. 2012;125:2407–2415.
20. Serbulea V, DeWeese D, Leitinger N. The effect of oxidized phospholipids on phenotypic polarization and function of macrophages. *Free Radic Biol Med*. 2017;111:156–168.
21. Thimmulappa RK, Gang X, Kim JH, Sussan TE, Witztum JL, Biswal S. Oxidized phospholipids impair pulmonary antibacterial defenses: evidence in mice exposed to cigarette smoke. *Biochem Biophys Res Commun*. 2012;426:253–259.
22. Knapp S, Matt U, Leitinger N, van der Poll T. Oxidized phospholipids inhibit phagocytosis and impair outcome in gram-negative sepsis in vivo. *J Immunol*. 2007;178:993–1001.
23. Stettner S, Ledwozyw A. Betamethasone and adult rat lung surfactant lipids. *Acta Vet Hung*. 1995;43:291–296.
24. Pollreisz A, Afonyushkin T, Oskolkova OV, Gruber F, Bochkov VN, Schmidt-Erfurth U. Retinal pigment epithelium cells produce VEGF in response to oxidized phospholipids through mechanisms involving ATF4 and protein kinase CK2. *Exp Eye Res*. 2013;116:177–184.
25. McIntyre TM. Bioactive oxidatively truncated phospholipids in inflammation and apoptosis: formation, targets, and inactivation. *Biochim Biophys Acta*. 2012;1818:2456–2464.
26. Forrester JV, Huitinga I, Lumsden L, Dijkstra CD. Marrow-derived activated macrophages are required during the effector phase of experimental autoimmune uveoretinitis in rats. *Curr Eye Res*. 1998;17:426–437.
27. Robertson MJ, Erwig LP, Liversidge J, Forrester JV, Rees AJ, Dick AD. Retinal microenvironment controls resident and infiltrating macrophage function during uveoretinitis. *Invest Ophthalmol Vis Sci*. 2002;43:2250–2257.

Investigative Ophthalmology & Visual Science